Reduced drag coefficient for high wind speeds in tropical cyclones

Mark D. Powell*, Peter J. Vickery† & Timothy A. Reinhold‡

* *National Oceanic and Atmospheric Administration, Atlantic Oceanographic and Meteorological Laboratory, Hurricane Research Division, Miami, Florida 33149, USA*
† *University of Western Ontario, Boundary Layer Wind Tunnel, London, Ontario N6A 5B9, Canada*
‡ *Clemson University, Department of Civil Engineering, Clemson, South Carolina 29634, USA*

The transfer of momentum between the atmosphere and the ocean is described in terms of the variation of wind speed with height and a drag coefficient that increases with sea surface roughness and wind speed. But direct measurements have only been available for weak winds; momentum transfer under extreme wind conditions has therefore been extrapolated from these field measurements. Global Positioning System sondes have been used since 1997 to measure the profiles of the strong winds in the marine boundary layer associated with tropical cyclones. Here we present an analysis of these data, which show a logarithmic increase in mean wind speed with height in the lowest 200 m, maximum wind speed at 500 m and a gradual weakening up to a height of 3 km. By determining surface stress, roughness length and neutral stability drag coefficient, we find that surface momentum flux levels off as the wind speeds increase above hurricane force. This behaviour is contrary to surface flux parameterizations that are currently used in a variety of modelling applications, including hurricane risk assessment and prediction of storm motion, intensity, waves and storm surges.

In strong winds, momentum exchange at the sea surface is described by a sea-state-dependent drag coefficient (C_d). The behaviour of C_d in tropical cyclones has never been observed, so it is currently based on extrapolations from field measurements in much weaker wind regimes. These extrapolations describe an increase in C_d with wind speed and are currently employed in applications such as: forecasting the intensity and track of tropical cyclones in numerical weather prediction models[1]; diagnosing surface wind speeds from reconnaissance flight-level observations[2,3]; determining the geographic distribution of extreme wind loads and loss with probabilistic models[4] for building design and insurance ratemaking, respectively; and specification of the wind field forcing for storm surge[5,6] and wave forecasts[7].

Under neutral stability in strong winds, the vertical variation of mean wind speed is controlled by the roughness of the sea surface. Relevant surface layer quantities are sea surface roughness length (Z_0), friction velocity (U_*), and the neutral stability 10-m wind speed (U_{10}) and drag coefficient (C_d). Assuming a neutrally stable surface layer, the mean wind speed (U) increases logarithmically[8] with height (Z).

$$U = (U_*/k)\ln(Z/Z_0) \quad (1)$$

where k is a constant of about 0.4, and U_* is the friction velocity related to the surface momentum flux (τ)

$$\tau = \rho U_*^2 = \rho C_d U_{10}^2 \quad (2)$$

and ρ is the air density. The roughness length described by Charnock[9] is:

$$Z_0 = \alpha U_*^2/g \quad (3)$$

where α is a constant of range 0.015–0.035. Estimates of U_*, Z_0 and C_d are computed by measurement of the momentum flux using eddy correlation and inertial dissipation methods or by using the mean wind speed profile with equations (1) and (2).

Field studies based primarily on eddy correlation and inertial dissipation measurements have examined C_d and Z_0 dependence on U_{10} and sea state in winds below hurricane force[10–15]. Indirect estimates of C_d for hurricanes[16–18] have been made from angular momentum and vorticity budgets, but errors are large. C_d depends on Z_0, U_{10}, wave age (ratio of local friction velocity to phase speed of dominant spectral component) and wave steepness[19–22]. Influences on Z_0 include steepness of wind waves, surface current velocity, and relative directions of wind, waves, current and swell. These studies suggest that swell and wind waves from different directions and fetches modulate the local Z_0 independently of U_{10}. Individual waves may distort the overlying wind field[23] by setting up speed-up and separation zones over and to leeward of the wave crest, respectively. Estimates of the vertical extent of this effect range from a few centimetres[24] to three wave heights[25].

Recent measurements of directional wave spectra[26] gathered by NOAA research aircraft in Hurricane Bonnie of 1998 depict the classic conceptual model[27] with the longest and largest (shortest and smallest) waves in the right front (left rear) quadrant, but show a complex pattern with multiple wave modes propagating at large and sometimes conflicting angles to the local wind, with a tendency for steeper waves in the right rear quadrant.

Wind measurement by GPS sonde

High-resolution wind profile measurements are now possible owing to the development of the Global Positioning System dropwindsonde (GPS sonde)[28]. From 1997–1999, 331 wind profiles were measured in the vicinity of the hurricane eyewalls in the Atlantic, and Eastern and Central Pacific basins (Table 1). The eyewall contains the strongest winds of a tropical cyclone and is identified as the ring of convection typically surrounding the relatively clear 'eye' depicted in satellite and radar imagery.

The GPS sonde is launched from reconnaissance or research aircraft at altitudes of 1.5–3 km or higher and falls at a vertical speed of 10–15 m s^{-1}, while sampling pressure, temperature, humidity and position every 0.5 s. A sonde launched in the eyewall takes several minutes to reach the surface while drifting (relative to the storm centre) tangentially 10–15 km and radially hundreds of metres. Wind speeds calculated from the motion of the GPS sonde have an accuracy of 0.5–2.0 m s^{-1}, and height is typically estimated to within 2 m. GPS sonde measurements were smoothed by a 5-s low-pass filter to remove fluctuations associated with undersampled scales and noise due to satellite switching. Extreme

© 2003 Nature Publishing Group

turbulence and intense rainfall contribute to signal interruptions or failures of GPS sondes to report values all the way to splash at the sea surface. Limited comparisons of GPS sondes to NOAA moored buoy and Coastal-Marine Automated Network platform observations[29] suggest GPS sonde winds are within 3.5 m s^{-1} of nearby buoy measurements at moderate wind speeds.

Wind profiles were examined in a composite sense (as a normalized profile containing all measurements gathered in the lowest 3 km), and also as a function of mean boundary layer (MBL) wind speed. For the MBL analysis, individual profiles were organized into five groups according to the MBL wind speed, defined as the mean wind speed of all profile observations below 500 m. The five groups corresponded to MBL wind speeds in the ranges of 30–39 m s^{-1} (72 profiles), 40–49 m s^{-1} (105 profiles), 50–59 m s^{-1} (55 profiles), 60–69 m s^{-1} (61 profiles) and 70–85 m s^{-1} (38 profiles). Near-surface (8–14 m) winds sampled by the GPS sondes ranged from 21 to 67 m s^{-1}. Each group was ordered vertically into height bins chosen to provide the highest resolution where the wind shear is the greatest. Variability associated with mesoscale, convective, and undersampled turbulent scales was removed by averaging all profiles in a given wind speed group.

Wind profile scaling

Scaled winds and heights were considered for constructing a normalized wind profile. A scaling height quantity was not selected because of the lack of a consistent objective method for estimating boundary layer height (thus the arbitrary definition of MBL) and variability or uncertainty of other possible quantities, including depth of the inflow layer, gradient wind level and height of the maximum wind speed. Planetary boundary layer (PBL) scaling heights determined from potential temperature or specific humidity mixed layer depths could differ by a factor of two.

The 'gradient' wind level is frequently used in engineering applications to represent the height at which the 'free atmosphere' flows above the boundary layer. Ideally, the gradient wind flows parallel to lines of constant pressure (isobars) and represents the source of momentum that can be transported to the surface in gusts. A 'gradient height' is difficult to assign in a tropical cyclone, because 'gradient balance'[30] may apply to winds as high as 3 km above the surface. A gradient height based on zero inflow (assuming inflow represents frictional surface effects of the PBL) yields values 1–3 km above thermodynamic measures of boundary layer height.

The MBL was selected to normalize the wind measurements because it usually contains the maximum wind speed measured in the profile, is not greatly affected by multiple maxima and minima, and also contains all the boundary layer measurements. The MBL wind was within 10% of the maximum mean wind in all groupings, so it was consistent with the concept of a 'gradient' wind as a source of momentum for gusts affecting the surface.

Table 1 **GPS sonde wind profiles in tropical cyclones**

Storm	Year	Profiles	Tropical storm	Cat1	Cat2	Cat3	Cat4	Cat5
Bonnie	1998	84	–	0	84	0	0	0
Bret	1999	11	–	0	1	3	7	0
Danielle	1998	4	–	4	0	0	0	0
Dennis	1999	32	2	8	22	0	0	0
Dora	1998	8	–	4	3	1	0	0
Erika	1997	22	–	0	0	22	0	0
Eugene	1999	1	–	1	0	0	0	0
Floyd	1999	58	1	4	10	20	23	0
Georges	1998	22	–	0	0	9	13	0
Gert	1999	7	–	0	1	0	6	0
Guillermo	1997	6	–	0	0	6	0	0
Irene	1999	2	–	0	2	0	0	0
Jose	1999	1	–	0	1	0	0	0
Lenny	1999	22	–	5	3	6	8	0
Mitch	1998	51	–	0	3	5	37	6
Totals		331	3	26	130	72	94	6

Number of individual GPS sonde wind profiles in tropical cyclones by storm and by Saffir–Simpson damage potential scale category (Cat) as determined by the National Hurricane Center 'best track'.

Mean wind profile

The normalized composite wind profile in Fig. 1 contains all (over 126,000) individual 0.5-s samples from 331 profiles comprising all MBL groups. The lower 200 m of the profile shows a logarithmic increase of mean wind speed with height, reaching a maximum near 500 m. Wind speeds decreased above 500 m owing to the weakening of the horizontal pressure gradient with height in the warm core of the hurricane[31,32]. Increased variability of the individual wind measurements above 600 m contradicts the concept of a 'free atmosphere' flow above the PBL.

Most of this variability is probably caused by convective scale features in the eyewall as well as the location of the GPS sonde launch relative to the flight-level wind maximum. The outward tilt of angular momentum surfaces with height[33] (eyewall tilt) places the location of the maximum wind at typical launch altitudes (3 km) as much as 1–3 km radially outward (relative to the storm centre) from the location of the maximum wind at the surface. GPS sondes launched radially outward from the 3-km wind maximum would fall into weaker MBL winds, whereas those launched radially inward from the 3-km maximum would tend to fall into stronger MBL winds.

Estimation of surface winds and gusts

The relationship of the surface and typical flight-level winds to the MBL can be used to estimate surface winds based on reconnaissance flight-level wind measurements. U_{10} is about 78% (standard deviation 8%) of the MBL. The 1.5-km flight-level wind is about equal (13%) to the MBL for MBL groups $<$60 m s^{-1}, and then decreases to 96% (12%) and 93% (10%) for the 60–69 and 70–85 m s^{-1} MBL groups, respectively. The ratio of the 3-km flight-level wind to the MBL decreases from 110% (37%), to 97% (20%), to 90% (14%), to 87% (12%) and to 84% (11%) as the MBL wind speed group

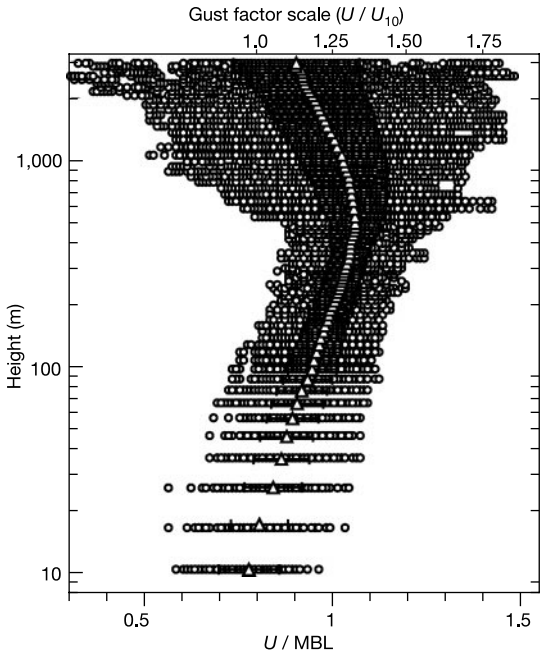

Figure 1 GPS sonde wind speed measurements normalized by mean boundary layer wind. Individual measurements (open circles), mean (open triangles) and standard deviation (horizontal bars) are shown for each height bin. An alternative scale of U/U_{10} is also shown, to represent the surface gust factor.

© 2003 Nature Publishing Group

increases successively from 30–39 to 70–85 ms^{-1}.

It must be stressed that these factors are only relevant for deep-water, open-ocean conditions. A variety of field experiments conducted in shallow water with shoaling waves suggest that higher roughness (and smaller surface wind reduction factors) would be experienced adjacent to coastal areas. This is of special concern now that GPS sonde information is influencing a reanalysis of the major US hurricane landfalls (for example, http://www.noaanews.noaa.gov/stories/s966.htm). Such reassessments are premature until sufficient numbers of GPS sonde profiles become available to distinguish between open-ocean conditions and shoaling and breaking wave effects in coastal areas.

The ratio of the surface wind to MBL was used to create an 'alternative' gust factor scale (ratio of the individual wind speed measurements to the mean surface wind speed) in Fig. 1. For mean winds above 25 m s^{-1} observed by coastal anemometers during hurricane landfall[34], gust factors (ratio of the peak 3-s gust to the 10-min mean) average at 1.5 with the largest gust factors at about 1.8. For marine exposure winds over 25 m s^{-1}, the mean gust factor[35] is around 1.4. Convective gusts[36,37] are believed to represent the transport and acceleration of extreme winds to the surface through downdrafts with gust factors of over 2.0. Observations of convective gusts in tropical cyclones are extremely rare because power outages and anemometer failures make it difficult to preserve continuous wind speed records. The highest wind observations at 10 m in Fig. 1 suggest gust factors less than 1.3, which is in agreement with values measured by NOAA buoy platforms in hurricanes. Examination of tropical cyclone anemometer records typically shows peak gust values of the order of three standard deviations in excess of the mean. The envelope of minima and maxima in Fig. 1 may, however, not be comparable to lulls and gusts measured by conventional anemometers, because filtering during post-processing effectively smoothes out high-frequency fluctuations.

Drag coefficient and surface roughness

Analysis of eyewall thermodynamic soundings[38] document well-mixed layers of potential temperature and specific humidity consistent with well-developed boundary layers. Mean wind profiles for each MBL group (Fig. 2) were logarithmic in the lowest 200 m and then levelled off slightly with a peak near 500 m. The log profile is consistent with a neutral stability surface layer in which the vertical distribution of momentum is controlled by surface roughness, as described by equation (1). The profiles suggest a decrease in the elevation of the maximum mean wind as the MBL wind speed increases. This behaviour is consistent with a shallower boundary layer in stronger storms.

The lowest 100–150 m of each MBL group in Fig. 2 was fitted by a least-squares line to determine the intercept (on a natural log height scale) and slope as a measure of Z_0 and k/U_* respectively, according to equation (1). The drag coefficient was computed from equation (2). Values of U_*, Z_0 and C_d for four estimates of surface layer depth are shown in Fig. 3. The 10–150-m layer tended to have the smallest error bars. All fits explained over 98% of the variance.

The group in the range 70–85 m s^{-1} contained too few low-level samples to determine reliable estimates of slope and intercept. Surface layer parameter dependence on wind speed (Fig. 3) showed that U_* increased with U_{10} up to 40 m s^{-1} before levelling off, and that Z_0 and C_d initially increased as surface winds approached hurricane force (33 m s^{-1}). For $U_{10} < 40$ m s^{-1}, U_* and Z_0 behaviour (Fig. 3a, b) was very similar to that described by Large and Pond[13], although Z_0 decreased with $U_{10} > 40$ m s^{-1} and the Z_0 values became much less than those predicted by the Charnock[9] and Large and Pond relationships. The magnitudes of C_d (Fig. 3c) for $U_{10} < 40$ m s^{-1} were consistent with numerous investigations[39], several budget studies conducted in tropical cyclones, and recent flume and annulus experiments (M. A. Donelan, personal communication; see also ref. 40), although the tendency was for a decrease in C_d for $U_{10} > 33$ m s^{-1}. The most remarkable result was the large decrease in Z_0 and C_d as U_{10} increased to 51 m s^{-1}, which was not indicated by any of the investigations shown in Fig. 3c. However, no observations previously existed for such wind speeds (the values shown from previous investigations are extrapolations).

A possible explanation for the transition in Z_0 and C_d as U_{10} increased from 40 to 51 m s^{-1} is the development of a sea foam layer[41] at the air–sea interface. Surface winds above hurricane force (34 m s^{-1}) create streaks of bubbles on the sea surface combined with patches of foam 20–50 m wide caused by steep wave faces breaking and being sheared off by the wind (Fig. 4a). As the wind approaches 50 m s^{-1}, the sea becomes completely covered by a layer of foam and it is difficult to discern individual wave-breaking elements in the reduced visibility from spray and rain (Fig. 4b). Experiments with a bubble annulus[42] suggest that bubble layers in salt water impede the transfer of momentum from the wind. As winds increase above 40 m s^{-1}, it is speculated that increased foam coverage could progressively form a 'slip' surface at the air–sea interface. In addition to the possible effects of foam, sea spray is

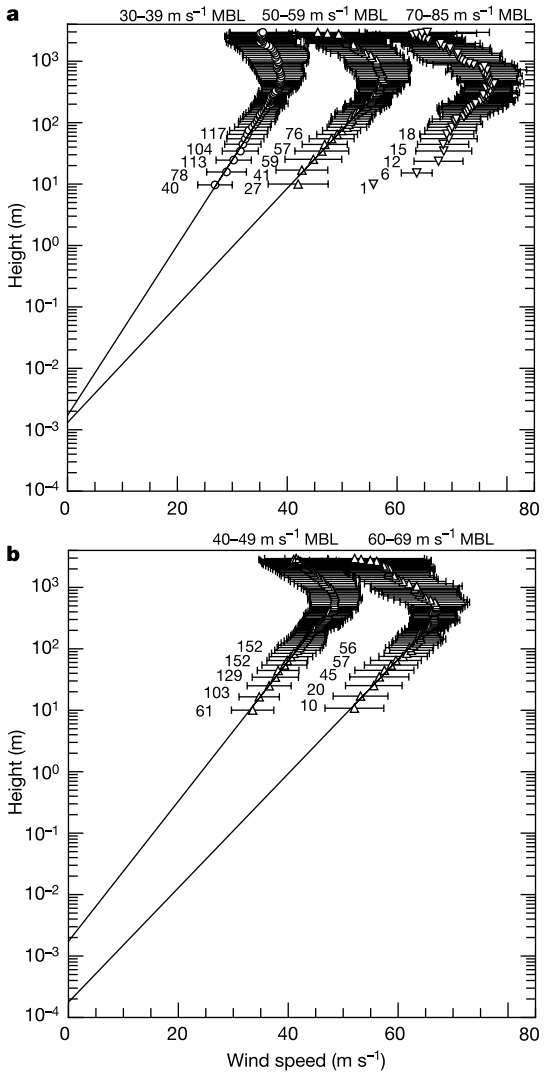

Figure 2 Mean wind profiles by MBL group. Symbols and horizontal bars represent mean and standard deviation for each vertical bin, numbers adjacent to each level represent the number of samples within each of the lowest five height bins. **a**, 30–39 m s^{-1} (72 profiles), 50–59 m s^{-1} (55 profiles) and 70–85 m s^{-1} (38 profiles) MBL groups. **b**, 40–49 m s^{-1} (105 profiles) and 60–69 m s^{-1} (61 profiles) MBL groups.

© 2003 Nature Publishing Group

hypothesized to significantly influence the transfer of momentum, heat and moisture in tropical cyclones[43].

Remote sensing measurements from the NOAA WP-3D aircraft[44] provide independent evidence supporting the C_d and Z_0 behaviour observed in the GPS sonde profiles. Scatterometer measurements of normalized radar cross-section (σ_0) due to Bragg scattering from surface capillary waves 'saturate' or fail to continue to increase at threshold wind speeds over 40 m s^{-1}. A levelling off of σ_0 with increasing U_{10} might be associated with the spacing and steepness of wind waves such that the wind 'sees' an effective surface that represents the tops of the separation zones between the waves (M. A. Donelan, personal communication). A reduction in C_d with increasing U_{10} is also supported by estimates of the angular momentum budget and the implied frictional dissipation in Hurricane Frederic[45] but the wind speeds were much less than those considered here. A field investigation of ocean response to Hurricane Gilbert[46] determined C_d from the near-inertial energy flux across the top of the oceanic thermocline. Although the C_d values exceeded those described here, a levelling-off behaviour is indicated.

An alternative scenario to describe the Z_0 and C_d behaviour implied by the mean profiles concerns speculation on the existence of linear coherent features in the form of helical rolls[47]. At low levels, GPS sondes could be preferentially drawn into a convergent and downward part of a helical roll circulation that would contain the strongest winds, contributing to a profile with smaller shear (and lower Z_0 and U_*) near the surface. Validation of such features will require simultaneous multiple Doppler radar measurements of the same sampling volume.

A final possible explanation for the shape of the mean wind profiles and resulting surface layer parameters involves sampling strategy. Most GPS sondes are launched strategically to place them near the surface wind maximum. They are usually dropped radially inward from the flight-level wind maximum. The GPS sonde trajectories are generally tangential until they reach the lowest 300–500 m, at which point the radial (inward relative to the storm centre) component of the wind increases. Hence, the GPS sonde

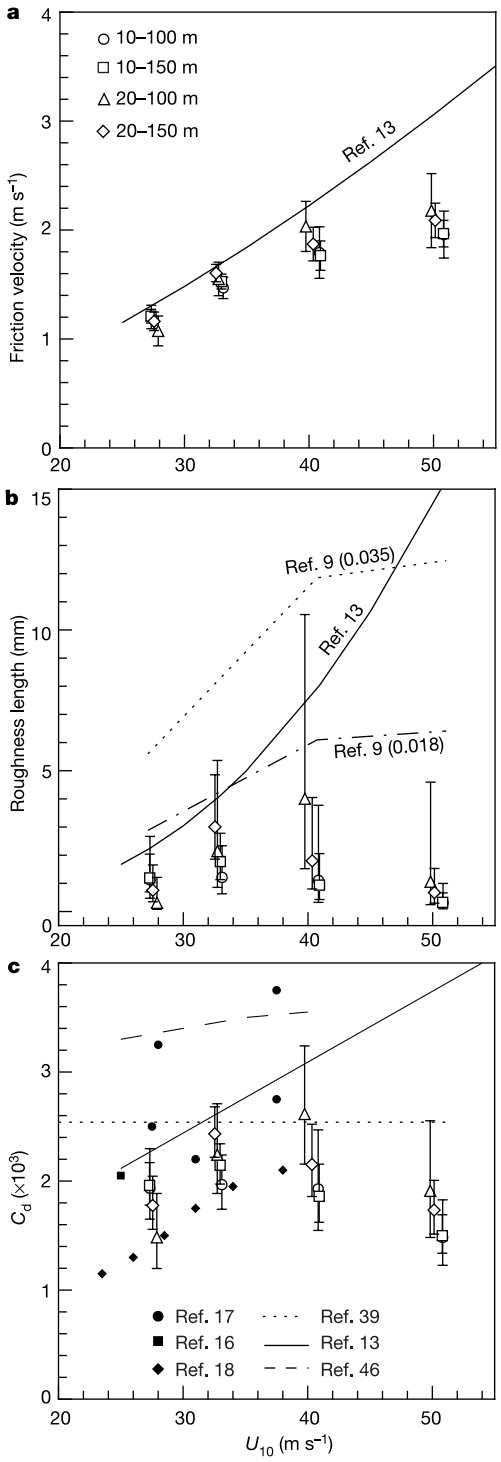

Figure 3 Surface momentum exchange quantities as a function of U_{10}. Vertical bars represent the range of estimates based on 95% confidence limits and symbols (see key in **a**) show estimates based on the depth of the surface layer used for the fit. **a**, U_*, from GPS sondes (symbols) and Large and Pond relationship[13] (solid line). **b**, Z_0 from GPS sonde profiles (symbols) with Large and Pond[13] (solid line) and Charnock[9] relationships for comparison (dotted line, $\alpha = 0.035$; dashed-dot line, $\alpha = 0.018$). **c**, C_d, with relationships and values from tropical cyclone budget studies[13,16–18,39,46].

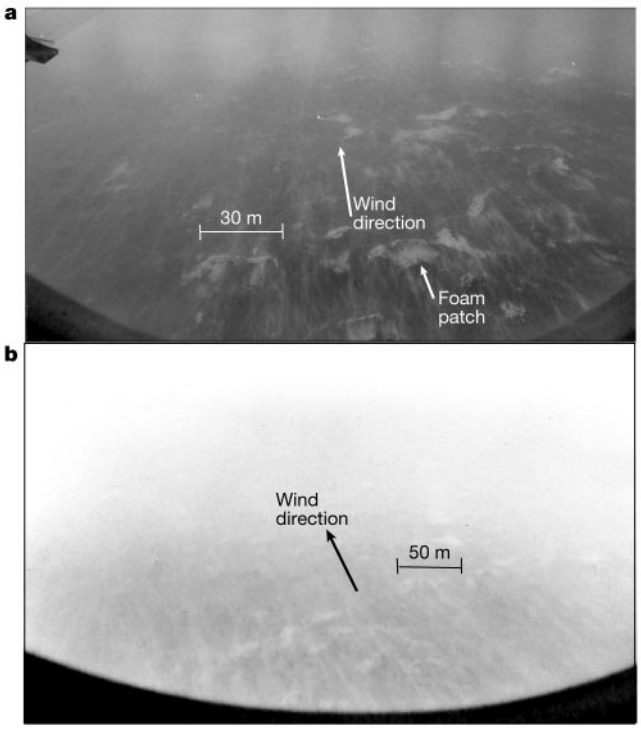

Figure 4 Sea state photographs during an eyewall penetration in Hurricane Ella on 1 September 1978. **a**, At 15:21 UTC (universal time coordinated) from 253-m altitude with flight-level wind speed of 46 m s^{-1} (starboard wing is at upper left). **b**, at 15:23 UTC from 450-m altitude with flight-level wind speed of 55 m s^{-1}. Arrows show the wind direction and scales suggest approximate sizes of wave features. Photographs taken by M.D.P. aboard the NOAA WP-3D research aircraft.

© 2003 Nature Publishing Group

may be moving horizontally towards the surface wind maximum, causing the reported winds to increase while falling closer to the surface (thus contributing to weaker wind shear). However, it seems just as likely that a GPS sonde could fall through the location of the surface wind maximum well before reaching the surface, and then be moving towards the relatively weak eye.

Until now, there have been no observations of wind profiles, surface stress, Z_0 and C_d in winds much above 25 m s^{-1}. Our findings provide compelling evidence that logarithmic mean wind profiles exist in tropical cyclones and that the surface stress, Z_0 and C_d are much less than previously thought in winds above 40 m s^{-1}. Heat and moisture transfer coefficients have a U_* dependence and may also be reduced. Such winds comprise less than 1% of a mature tropical cyclone's circulation, but have a crucial role in enhanced surface fluxes that supply enthalpy to the eyewall. The amount of enthalpy in the eyewall is directly related to the intensity of the tropical cyclone[48].

Surface layer parameterizations used in tropical cyclone motion, intensity, wave and storm surge prediction and risk assessment may not be valid in high wind, fetch-limited conditions over the open ocean. In the light of possible effects on heat and moisture transfer, shoaling effects in shallow water, and azimuth-dependent sea state and environmental wind-shear-induced asymmetries in the wind field, we consider that continued collection and examination of GPS sonde profiles is warranted. □

Received 18 September 2002; accepted 4 February 2003; doi:10.1038/nature01481.

1. Bender, M. A., Ginis, I. & Kurihara, Y. Numerical simulations of tropical cyclone–ocean interaction with a high-resolution coupled model. *J. Geophys. Res.* **98,** 23245–23263 (1993).
2. Powell, M. D. Evaluations of diagnostic marine boundary layer models applied to hurricanes. *Mon. Weath. Rev.* **108,** 757–766 (1980).
3. Powell, M. D. & Black, P. G. The relationship of hurricane reconnaissance flight-level wind measurements to winds measured by NOAA's oceanic platforms. *J. Wind Eng. Ind. Aerodyn.* **36,** 381–392 (1990).
4. Vickery, P. J., Skerlj, P. F., Steckley, A. C. & Twisdale, L. A. Hurricane wind field model for use in hurricane simulations. *J. Struct. Eng. ASCE* **126,** 1203–1222 (2000).
5. Jelesnianski, C. P., Chen, J. & Shaffer, W. A. SLOSH: Sea, Lake, and Overland Surges from Hurricanes. *NOAA Tech. Rep.* NWS 48 (1992).
6. Blain, C. A., Westerink, J. J. & Luettich, R. A. Jr The influence of domain size on the response characteristics of a hurricane storm surge model. *J. Geophys. Res.* **99,** 18467–18479 (1994).
7. Tolman, H. L. *et al.* Development and implementation of wind generated ocean surface wave models at NCEP. *Weath. Forecast.* **17,** 311–333 (2002).
8. Paulson, C. A. The mathematical representation of wind speed and temperature profiles in the unstable atmospheric surface layer. *J. Appl. Meteorol.* **9,** 857–861 (1970).
9. Charnock, H. Wind stress on a water surface. *Q. J. R. Met. Soc.* **81,** 639–640 (1955).
10. Garratt, J. R. Review of drag coefficients over oceans and continents. *Mon. Weath. Rev.* **104,** 418–442 (1977).
11. Donelan, M. A., Dobson, F. W., Smith, S. D. & Anderson, R. J. On the dependence of sea surface roughness on wave development. *J. Phys. Oceanogr.* **23,** 2143–2149 (1993).
12. Smith, S. D. Coefficients for sea surface wind stress, heat flux, and wind profiles as a function of wind speed and temperature. *J. Geophys. Res.* **93,** 15467–15472 (1988).
13. Large, W. G. & Pond, S. Open ocean momentum flux measurements in moderate to strong winds. *J. Phys. Oceanogr.* **11,** 324–336 (1981).
14. Taylor, P. K. & Yelland, M. J. The dependence of sea surface roughness on the height and steepness of the waves. *J. Phys. Oceanogr.* **31,** 572–590 (2001).
15. Vickery, P. J. & Skerlj, P. F. Elimination of exposure D along the hurricane coastline in ASCE 7. *J. Struct. Eng.* **126,** 545–549 (2000).
16. Palmen, E. & Riehl, H. Budget of angular momentum and energy in tropical cyclones. *J. Meteorol.* **14,** 150–159 (1957).
17. Miller, B. I. A study of the filling of Hurricane Donna (1960) over land. *Mon. Weath. Rev.* **92,** 389–406 (1964).
18. Hawkins, H. F. & Rubsam, D. T. Hurricane Hilda Part II: Structure and budgets of the hurricane on 1 Oct. 1964. *Mon. Weath. Rev.* **96,** 617–636 (1968).
19. Donelan, M. A. & Hui, W. H. *Surface Waves and Fluxes* (eds Geernaert, G. L. & Plant, W. J.) (Kluwer, Dordrecht, 1990).
20. Geernhart, G. L., Katsaros, K. B. & Richter, K. Variation of the drag coefficient and its dependence on sea state. *J. Geophys. Res.* **91,** 7667–7679 (1986).
21. Smith, S. D. *et al.* Sea surface wind stress and drag coefficients: the HEXOS results. *Bound. Layer Meteorol.* **60,** 109–142 (1992).
22. Anctil, F. & Donelan, M. A. Air–water momentum flux observations over shoaling waves. *J. Phys. Oceanogr.* **26,** 1344–1353 (1996).
23. Krugermeyer, L., Gruenewald, M. & Dunckel, M. The influence of sea waves on the wind profile. *Bound. Layer Meteorol.* **14,** 403–414 (1978).
24. Jansen, P. A. E. M. Wave induced stress and the drag of air flow over sea waves. *J. Phys. Oceanogr.* **19,** 745–754 (1989).
25. Large, W. G., Morzel, J. & Crawford, G. B. Accounting for surface wave distortion of the marine wind profile in low-level ocean storms wind measurements. *J. Phys. Oceanogr.* **11,** 2959–2971 (1995).
26. Wright, C. W. *et al.* Hurricane directional wave spectrum spatial variation in the open ocean. *J. Phys. Oceanogr.* **31,** 2472–2488 (2001).
27. Tannenhill, I. R. *Hurricanes* (Princeton Univ. Press, Princeton, 1944).
28. Hock, T. R. & Franklin, J. L. The NCAR GPS dropwindsonde. *Bull. Am. Meteorol. Soc.* **80,** 407–420 (1999).
29. Houston, S. H. *et al.* in *Preprints 24th Conf. Hurricanes Tropical Meteorol. (Fort Lauderdale, Florida, May 29–June 2)* 339 (American Meteorological Society, Boston, 2000).
30. Willoughby, H. E. Gradient balance in tropical cyclones. *J. Atmos. Sci.* **47,** 265–274 (1990).
31. Shaw, N. The birth and death of cyclones. *Geophys. Mem.* **2,** 213–227 (1922).
32. Haurwitz, B. The height of tropical cyclones and of the 'eye' of the storm. *Mon. Weath. Rev.* **63,** 45–49 (1935).
33. Jorgensen, D. P. Mesoscale and convective scale characteristics of mature hurricanes. II: Inner core structure of Hurricane Allen (1980). *J. Atmos. Sci.* **41,** 1287–1311 (1984).
34. Krayer, W. R. & Marshall, R. D. Gust factors applied to hurricane winds. *Bull. Am. Soc.* **73,** 613–617 (1992).
35. Vickery, P. J. & Skerlj, P. F. Hurricane gust factors revisited. *J. Struct. Eng.* (submitted).
36. Bradbury, W. M. S., Deaves, D. M., Hunt, J. C. R., Kershaw, R. & Nakamura, K. The importance of convective gusts. *Meteorol. Appl.* **1,** 365–378 (1994).
37. Powell, M. D., Dodge, P. & Black, M. L. The landfall of Hurricane Hugo in the Carolinas. *Weath. Forecast.* **6,** 379–399 (1991).
38. Powell, M. D., Reinhold, T. A. & Marshall, R. D. in *Proc. 10th Int. Conf. Wind Eng. (Copenhagen, 21–24 June)* (eds Larsen, A., Larose, G. L. & Livesey, F. M.) 307–314 (Balkema, Rotterdam, 1999).
39. Amorocho, J. & DeVries, J. J. A new evaluation of the wind stress coefficient over water surfaces. *J. Geophys. Res.* **85,** 433–442 (1980).
40. Alamaro, M., Emanuel, K., Cotton, J., McGillis, W. & Edson, J. in *Preprints 25th Conf. Hurricanes Tropical Meteorol. (San Diego, California, April 29–May 3)* 667 (American Meteorological Society, Boston, 2002).
41. Newell, A. & Zakharov, V. E. Rough sea foam. *Phys. Rev. Lett.* **69,** 1149–1151 (1992).
42. Lundquist, J. in *Abstracts Limnology and Oceanography: Navigating into the Next Century (Santa Fe, New Mexico, February 1–5)* Abstr. SS54WE1538S (American Society of Limnology and Oceanography, Waco, Texas, 1999).
43. Kepert, J. D., Fairall, C. W. & Bao, J. W. in *Air–Sea Fluxes: Momentum, Heat, and Mass Exchange* (ed. Geernaert, G. L.) 363–409 (Kluwer, Dordrecht, 1998).
44. Donnelly, W. J. *et al.* Revised ocean backscatter models at C and Ku band under high-wind conditions. *J. Geophys. Res.* **104,** 11485–11497 (1999).
45. Kaplan, J. & Frank, W. M. The large scale inflow-layer structure of Hurricane Frederic (1979). *Mon. Weath. Rev.* **121,** 3–20 (1993).
46. Shay, L. K. Upper ocean response to tropical cyclones. *RSMAS Tech. Note 99-003* (Univ. Miami, Rosenstiel School of Marine and Atmospheric Science, Florida, 1999).
47. Katsaros, K. B., Vachon, P. W., Liu, W. T., Black, P. G. *J. Oceanography* **58,** 137–151 (2002).
48. Wroe, D. R. & Barnes, G. M. Inflow layer energetics of Hurricane Bonnie (1998) near landfall. *Mon. Weath. Rev.* **131** (in the press, 2003).

Acknowledgements This paper is dedicated to the memory of R. Marshall. The assistance of F. Marks, the scientific and support staff of the NOAA Hurricane Research Division in Miami, and the NOAA Aircraft Operations Center in Tampa is appreciated. W. McGillis provided insight on the possible effect of sea foam on momentum transfer in tropical cyclones. Comments on an earlier version of the manuscript by E. Uhlhorn, F. Marks and R. Rogers are appreciated.

Competing interests statement The authors declare that they have no competing financial interests.

Correspondence and requests for materials should be addressed to M.P. (e-mail: Mark.Powell@noaa.gov).

© 2003 Nature Publishing Group